ELSEVIER

Physics of the Earth and Planetary Interiors 126 (2001) 43–57

PHYSICS OF THE EARTH AND PLANETARY INTERIORS

www.elsevier.com/locate/pepi

Beyond Néel's theories: thermal demagnetization of narrow-band partial thermoremanent magnetizations

David J. Dunlop*, Özden Özdemir

Geophysics, Department of Physics, University of Toronto, Toronto, Canada M5S 1A7

Received 25 October 2000; received in revised form 30 January 2001; accepted 7 February 2001

Abstract

Partial thermoremanent magnetization (pTRM) was imparted over a narrow temperature interval, $T = 370$–350°C, to a suite of crushed and annealed natural magnetite samples, ranging in grain size from ≈1 to 125–150 μm and in domain state from small pseudo-single-domain (PSD) to multidomain (MD). In this way, effectively a single blocking temperature, T_B, of pTRM was activated. Stepwise thermal demagnetization did not erase the pTRMs sharply at T_B, as for single-domain (SD) grains. Demagnetization began well below 350°C and continued above 370°C, with a median unblocking temperature, T_{UB}, close to 360°C. The largest grains deviated most from SD behavior. Their pTRM demagnetized over the entire interval from room temperature to the Curie point, in accordance with predictions for MD grains. In terms of the unblocking temperature distribution $f(T_{UB})$ or slope dM/dT of the thermal demagnetization curve, SD grains have a sharp spectrum, $T_{UB} = T_B$; MD grains were observed to have a broad, roughly symmetrical spectrum centered on T_B; and intermediate size grains in the PSD range had non-Gaussian spectra, combining a central peak near T_B with broad tails above and below T_B. In this respect, PSD grains display a superposition of SD and MD remanences, not a blend between the two. Practical implications of these observations are that Thellier's law of reciprocity ($T_{UB} = T_B$) will be increasingly violated as grain size increases in the PSD range. The low-T_{UB} part of $f(T_{UB})$ produces anomalously large demagnetization of NRM in low-temperature heating steps of Thellier-type paleointensity determinations and a sagging shape of the Arai plot. The high-T_{UB} part of $f(T_{UB})$ results in undemagnetized remanence at and above T_B in thermal demagnetization. Among pre-treatments designed to make remanence more SD-like in subsequent thermal cleaning, alternating field (AF) pre-cleaning sharpened $f(T_{UB})$ more effectively than low-temperature demagnetization for the 20 μm sample.

Keywords: Demagnetization; Remanence; Paleointensity; Partial TRM; Magnetite

1. Introduction

Many paleomagnetic cleaning techniques are based on Néel's (1949) theory of single-domain (SD) grains. For example, thermoviscous remagnetization at temperature T produces an overprint that is generally assumed to be erasable by reheating in zero field to a similar peak temperature, when allowance is made for the different time scales of natural and laboratory heating. The same assumption, that the unblocking temperature T_{UB} of natural remanent magnetization (NRM) matches the blocking temperature T_B of partial thermoremanent magnetization (pTRM), underlies the Thellier method of paleointensity determination. Failures of thermal cleaning or paleointensity experiments are often blamed on chemical alteration of samples. In many cases, however, the assumption that

* Corresponding author. Present address: Erindale College, University of Toronto at Mississauga, 3359 Mississauga Road North, Mississauga, Ont., Canada L5l 1C6. Tel.: +1-905-828-3968; fax: +1-905-828-5425.
E-mail address: dunlop@physics.utoronto.ca (D.J. Dunlop).

0031-9201/01/$ – see front matter
PII: S0031-9201(01)00243-6

pseudo-single-domain (PSD) grains are adequately described by SD theory may be at fault.

The purpose of the present study was to test the assumption $T_{UB} = T_B$ for a suite of magnetites ranging in size from ≈1 to 125–150 μm and in domain state from small PSD to multidomain (MD). It is well established that MD grains have "anomalous" thermal characteristics, with demagnetization beginning much below (Dunlop and Özdemir, 2000) and extending well above (Shcherbakova et al., 2000) T_B of the pTRM or viscous remanence (VRM) being treated. Studies of high-T_{UB} thermal demagnetization "tails" have a long history. The first experiments on synthetic magnetites and hematites of known grain size were carried out by Roquet (1954), who observed that a pTRM with upper blocking temperature T_B was completely demagnetized in zero field reheating to $T_{UB} = T_B$ if the intensity of the pTRM was weak compared to that of total TRM, but required zero field heating to the Curie point T_C if the pTRM intensity was relatively strong. Two effects are involved: first, turning 'on' a field $\boldsymbol{H}$ at T_B produces an instantaneous isothermal remanence (IRM) which increases in importance as H increases and can only be erased by zero-field heating above T_B; second, as T_B increases, pTRM intensity increases, while the available range of T_{UB} between T_B and T_C decreases.

The IRM effect, i.e. the dependence of pTRM tails on field strength H, was fully documented by Everitt (1961, 1962), and Dunlop and West (1969), who studied SD and small PSD size grains. They found small pTRM tails even for fields as weak as 0.2 mT, but did not consider them to be significant violations of Néel's theory.

The first study to document wholesale violation of the Thellier–Néel law $T_{UB} = T_B$ was that of Shaskanov and Metallova (1972). They demonstrated that the IRM contribution to pTRM was inadequate to explain the thermal tails which were universally observed in their samples. Bol'shakov and Shcherbakova (1979), using SD, PSD and MD size magnetites and hematites, showed that thermal tails are not universal, but are associated with MD grains. SD and PSD grains had small tails or none at all, for pTRM fields $H =$ 0.05–0.4 mT. Further experiments, by Middleton and Schmidt (1982), Dunlop (1983), Worm et al. (1988), Halgedahl (1993), McClelland et al. (1996), Dunlop et al. (1997), and Shcherbakova et al. (1996, 2000) have refined these findings and have shown they apply also to viscous remanence (VRM), while theoretical models of the phenomenon have been advanced by McClelland and Sugiura (1987), Shcherbakov et al. (1993), and McClelland and Shcherbakov (1995).

Unblocking below the blocking temperature, i.e. $T_{UB} < T_B$, has been less studied. Markov et al. (1983), and McClelland and Sugiura (1987) observed decay of pTRM during zero-field cooling below the lower blocking temperature and a small further decay in subsequent zero-field heating in magnetites of large grain size. Shcherbakova et al. (1996, 2000), Dunlop and Özdemir (2000), and Muxworthy (2000) have observed the same "low-T_{UB} tails" of pTRM and VRM for MD grains (in some cases, the MD nature of the remanence carriers was inferred from other magnetic data).

2. Samples and experiments

Five samples were selected from a larger suite of sized magnetites. The mean grain sizes are 1, 6, 20, 110 (range 100–125 μm) and 135 (range 125–150 μm). These samples were chosen because they span the range from small PSD to MD. The hysteresis properties (Table 1) are consistent with the domain states expected on the basis of grain size. The magnetites were produced by crushing millimeter size magnetite crystals from Bancroft, Ont. Size fractions were separated by sieving for the 110 and 135 μm samples and by centrifugal sorting in a dust analyzer for the others. The magnetites were dispersed (≈1 vol.%) in CaF_2 and sealed in evacuated quartz capsules. They were then annealed for 2–3 h at 700°C to relieve strains introduced by crushing and to ensure a reproducible initial state for thermal experiments.

Table 1
Ratios of saturation remanence to saturation magnetization, M_{rs}/M_s, and remanent coercive force to ordinary coercive force, H_{cr}/H_c, for the experimental samples

Grain size, d (μm)	M_{rs}/M_s		H_{cr}/H_c	
	Unannealed	Annealed	Unannealed	Annealed
1	0.182	0.088	1.95	3.11
6	0.110	0.065	2.57	3.47
20	0.053	0.036	3.55	4.36
110	0.019	0.016	7.10	9.47
135	0.012	0.012	8.50	11.6

There are two experimental ways of isolating a single blocking temperature, T_B. A VRM produced by a few hours application of a small field $\boldsymbol{H}$ at temperature T will activate only those domains, domain walls, or other spin structures with $T_B \approx T$. A partial TRM produced by quick cooling in $\boldsymbol{H}$ from T_1 to T_2 will activate blocking temperatures in this range and none outside it. These are essentially definitions of what we mean by blocking temperature, not extrapolations of Néel's single-domain theory. The only complication is the possibility that a wall, wall segment, spin vortex, etc. may have more than one blocking temperature if conditions change during cooling, for example if a new wall nucleates (Halgedahl, 1991). Multiple T_B's are unlikely if (T_1, T_2) is narrow.

In this study, narrrow-band pTRM was produced by applying a field of either 0.3 or 0.5 mT over the interval (370, 350°C). This interval was chosen because in the SD limiting case, Néel's theory predicts that the pTRM would be equivalent to VRM produced over 3.5 h at 350°C; VRM produced under these conditions was used in previous work (Dunlop and Özdemir, 2000). We have no firm theory of VRM and pTRM for PSD grains, but the analogy between the two has some experimental support (Dunlop and Özdemir, 2000, Fig. 2). The initial state for all narrow-band pTRMs was alternating field (AF) demagnetized.

Thermal demagnetization was carried out in stepwise fashion, the common practice in paleomagnetism. Samples were heated and cooled in zero field in a six-layer mu-metal shield enclosing a water-cooled non-inductive furnace. A solenoid wound on the water jacket of the furnace was used to apply small fields for pTRM or VRM production. All remanence measurements were made with a 2 G superconducting magnetometer after cooling samples to room temperature.

3. The unblocking temperature spectrum $f(T_{UB})$ and a VRM example

A thermal demagnetization curve integrates over the distribution of unblocking temperatures T_{UB} in a sample. Conversely, the point-by-point slope dM/dT of a thermal demagnetization curve gives the unblocking temperature spectrum, $f(T_{UB})$. Although, the two representations of the data are equivalent, $f(T_{UB})$ reveals features such as the width and shape of the distribution more directly and clearly.

Thermal demagnetization data were numerically differentiated between limits of 95 and 5% of initial remanence. The area under each spectrum illustrated thus represents the central 90% of the remanence distribution. This truncation makes it easier to view and appreciate the essential features of the distributions.

Fig. 1 illustrates the contrasting spectra obtained from the thermal demagnetization of VRM for 0.04 μm (SD), 20 μm (PSD) and 135 μm (MD) magnetites (the thermal demagnetization data are from Dunlop and Özdemir (2000, Fig. 1)). Each distribution is

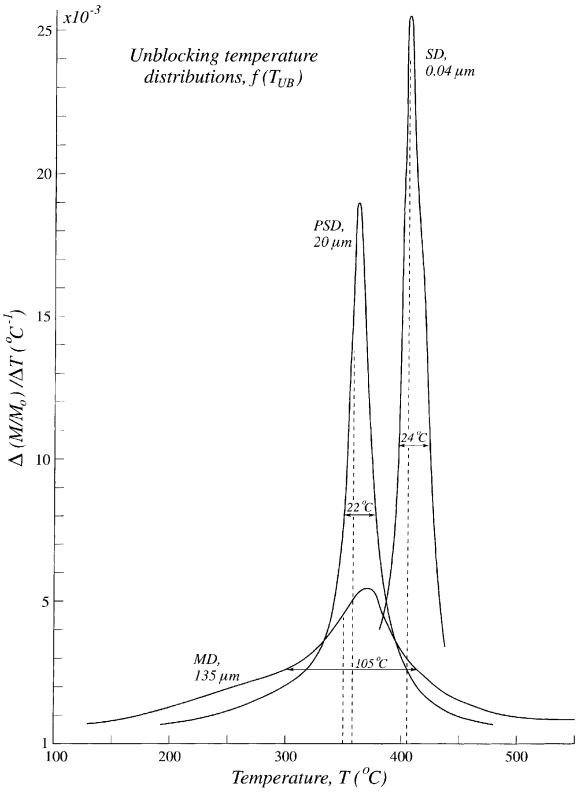

Fig. 1. Unblocking temperature distributions $f(T_{UB})$ obtained by numerically differentiating thermal demagnetization curves of VRMs for three magnetite samples, of SD, PSD and MD sizes. Vertical dashed lines indicate the blocking temperature T_B at which each VRM was acquired. The T_{UB} distributions are roughly symmetric about T_B. Data for the 0.04 μm SD sample have been scaled down by 0.75 for easier comparison with the other data. The distributions are truncated at lower and upper limits of 95 and 5% of initial remanence. The PSD (20 μm) spectrum combines a sharp SD-like central peak and broad MD-style tails.

approximately symmetric. The peak of each spectrum is somewhat above the temperature T at which VRM was produced (vertical dashed lines). Because of the joint effect of time and temperature, VRM produced at T activates short-term blocking temperatures $T_B > T$. When this effect is taken into account, the peak and median T_{UB} values agree well with the mean value of T_B on a short time scale for the SD and PSD samples. For the 135 μm MD sample, the mean T_{UB} is ≈10°C higher than the mean T_B.

Therefore, although a single T_B can generate a distribution of T_{UB}'s with both low- and high-temperature tails, the mean T_{UB} value matches T_B quite closely, for these data sets at least. The high-temperature demagnetization tail familiar from the work of Bol'shakov and Shcherbakova (1979), and Worm et al. (1988) is matched by a low-temperature demagnetization tail of about equal size. The key to detecting low-temperature tails is to isolate single values of T_B via VRM or narrow-band pTRMs and to begin thermal demagnetization immediately above room temperature T_0. Most previous work has missed the low-T_{UB} part of the spectrum by either beginning thermal demagnetization at T_B or using broad-band pTRMs with a lower temperature of T_0, in which the low-T_{UB} tails of many different T_B fractions are mingled and unresolved.

A feature not obvious in the starting thermal demagnetization data is the interesting shape of the PSD spectrum. It combines a narrow central peak, whose width is similar to that of the SD peak, with tails almost as broad as those of the MD spectrum. The PSD spectrum is not intermediate in a continuum between SD and MD end members. Rather it is a superposition of two distinct spectra, implying the coexistence of structures with SD and MD thermal responses in grains of a particular size.

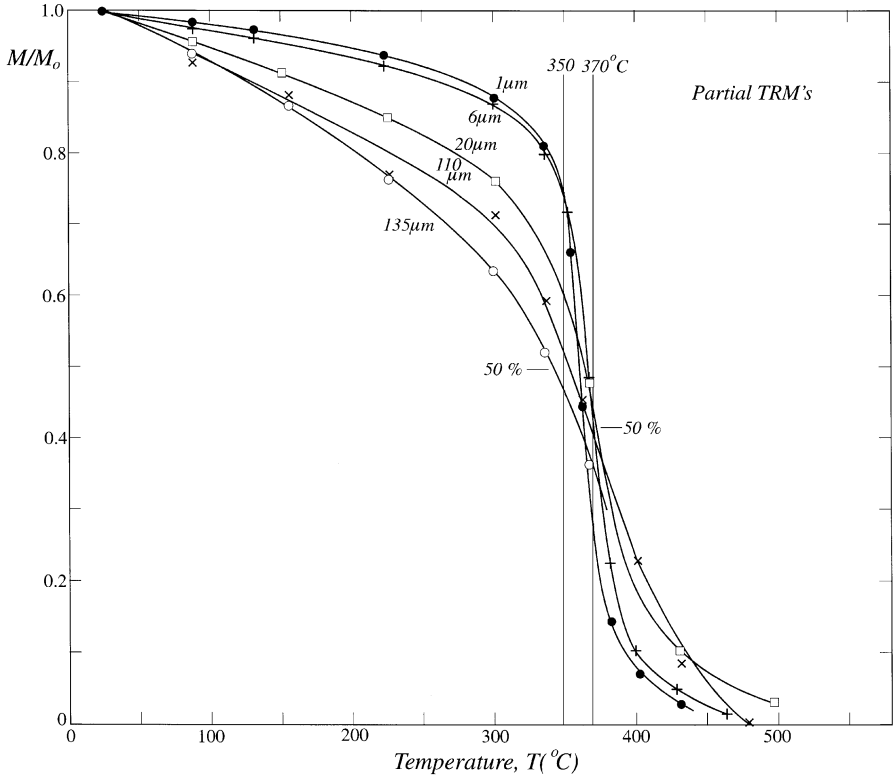

Fig. 2. Stepwise thermal demagnetization of pTRMs produced by a small field applied during cooling from 370 to 350°C in magnetites ranging from small PSD to MD size. About 50–90% of the remanence unblocks at temperatures below or above the pTRM blocking temperature range. These "anomalously" low or high T_{UB}'s are most important for the largest grains, but are appreciable even for the smallest PSD grains.

4. Thermal demagnetization of pTRMs as a function of grain size

Partial TRMs produced between 370 and 350°C in magnetites of varying grain sizes have a distinctive progression of thermal demagnetization curves (Fig. 2). The broad, almost uninflected curves of the 110 and 135 μm magnetites evolve to curves that are quite sharply inflected near the upper and lower bounds of the blocking range for the 1 and 6 μm samples. Unblocking temperatures lower than T_B are prominent for all grain sizes. About one-half of the remanence of the 110 and 135 μm magnetites and about one-quarter of the remanence of the 1 and 6 μm magnetites demagnetizes below 350°C. Tailing of thermal demagnetization curves is not confined to

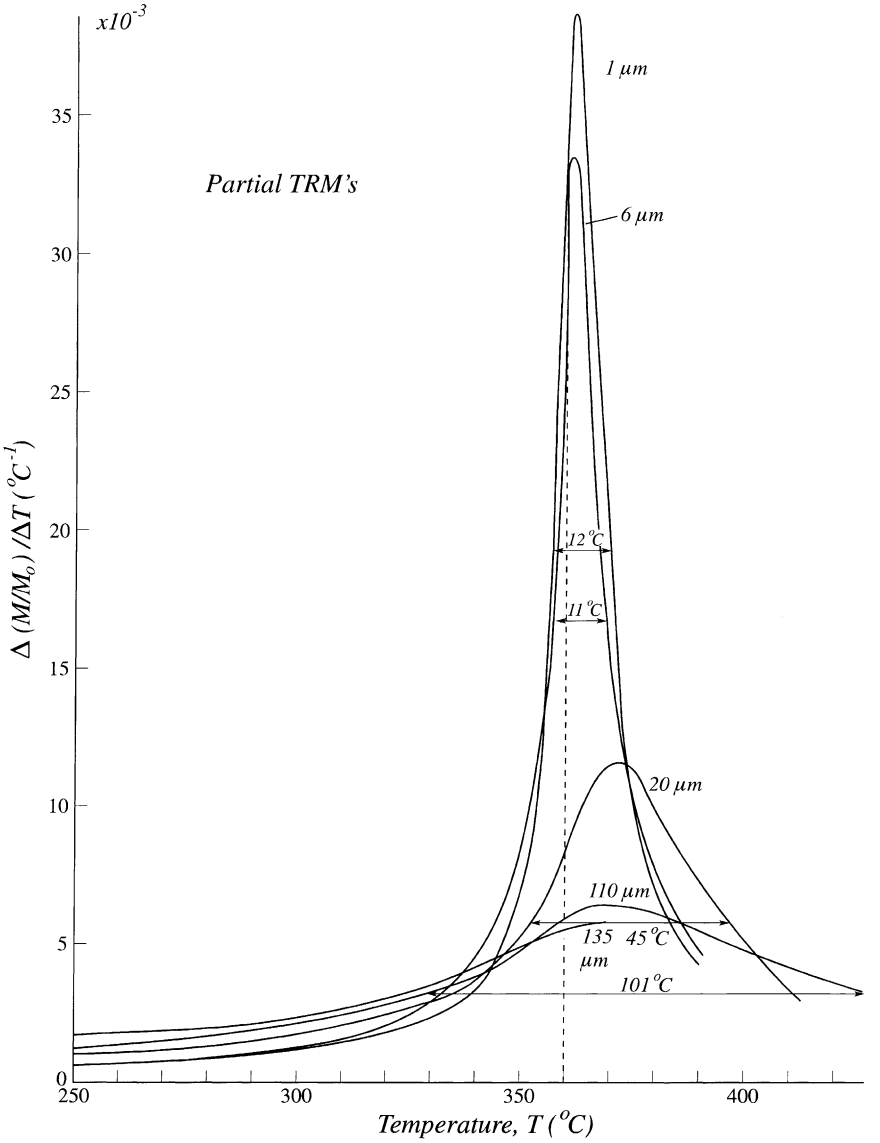

Fig. 3. Unblocking temperature distributions $f(T_{UB})$ obtained by numerically differentiating the pTRM thermal demagnetization curves of Fig. 2. The half-width of the spectrum for 110 μm MD grains is about an order of magnitude larger than the half-widths for 1 and 6 μm PSD grains.

large MD grains but is significant even for fairly small PSD grains.

The $f(T_{UB})$ distributions obtained by differentiating the thermal demagnetization curves appear in Fig. 3. All the distributions peak close to the mean T_B of 360°C but their shapes are quite different. The 110 μm spectrum is broad, with a half-width of ≈100°C, while the 1 and 6 μm spectra are sharply peaked, with half-widths of ≈10°C. Despite the SD-like central peaks, the 1 and 6 μm distributions tail off to low T_{UB}'s in a definitely non-Gaussian fashion. These PSD spectra are a superposition of sharp SD and broad MD spectra, not a blend between them.

5. Effects of $T_{UB} < T_B$ and $> T_B$ on paleointensity determination

In the modified Thellier method of paleointensity determination in general use today, a sample is heated twice to temperature T_n. The first heating and cooling, in zero field, are intended to demagnetize all of the natural remanent magnetization (NRM) with $T_B \leq T_n$. The second heating and cooling, in a laboratory field which ideally is adjusted to match the paleofield, are intended to produce a pTRM that restores the NRM fraction lost in the first step. For SD grains, since T_{UB} in the demagnetization step is exactly equal to T_B in the second step, the pTRM gained does equal the NRM lost. The Arai plot of NRM remaining versus pTRM gained is a straight line with the ideal SD slope of −1 (Fig. 4, upper dashed line).

For MD grains, the internal demagnetizing field is balanced by an external field in the cooling and acquisition of NRM, but is unbalanced in zero-field heating. It causes new domain walls to nucleate and existing walls to make a series of jumps towards a demagnetized state, beginning immediately above T_0 and extending up to and above T_B. The abundant low T_{UB}'s evident in the thermal demagnetization curves

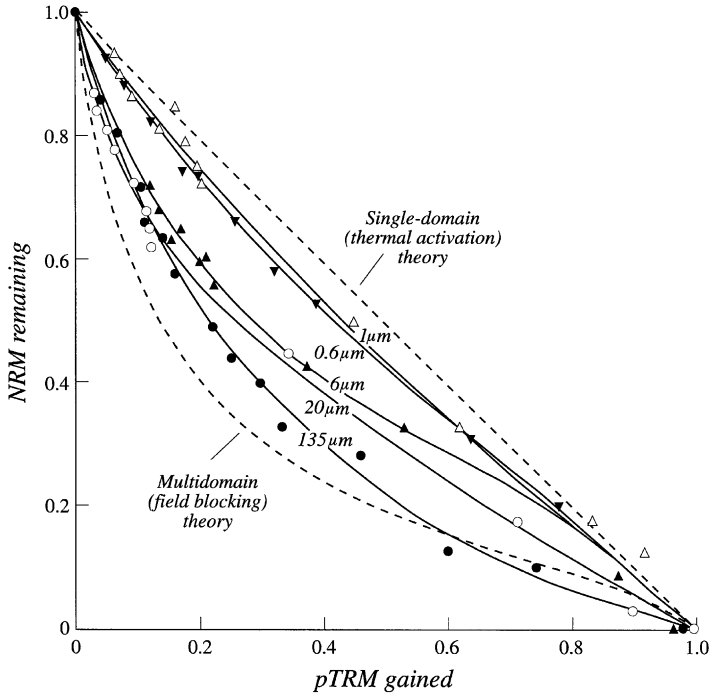

Fig. 4. Thellier paleointensity experiments simulated by using a laboratory TRM in place of NRM (after Dunlop (1998)). For all grain sizes, unblocking of "NRM" in low-temperature steps outweighs acquisition of pTRM at the same temperature, an expression of the tail of "anomalously" low T_{UB}'s in $f(T_{UB})$ for all grain sizes seen in Fig. 3. The result is sagging of the pseudo-paleointensity data below the ideal SD line (upper dashed curve) toward the MD curve (lower dashed curve) predicted by the theory of Dunlop and Xu (1994), and Xu and Dunlop (1994).

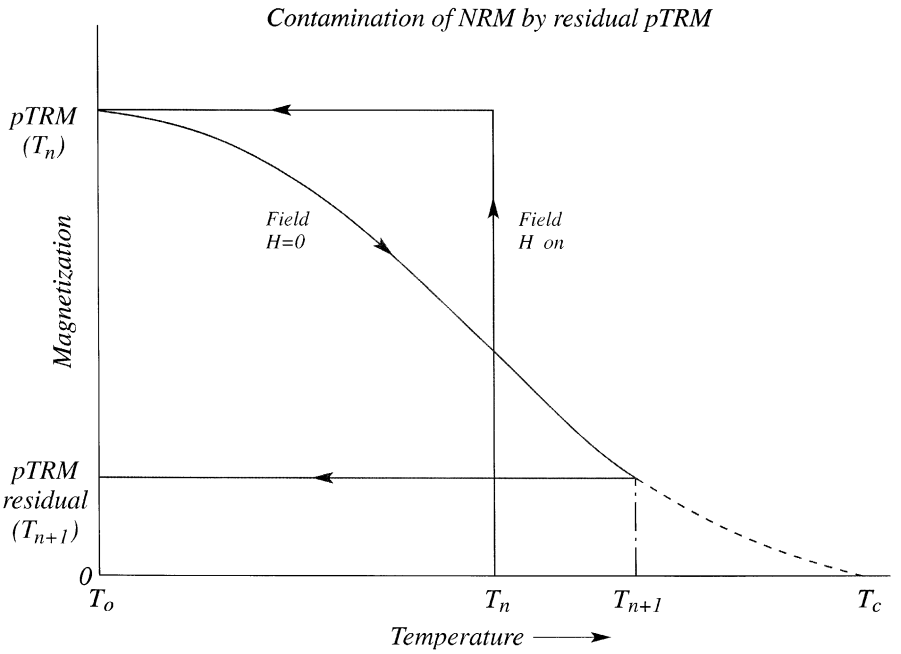

Fig. 5. Cartoon showing how pTRM acquired sharply in cooling below T_n (field H on: second heating/cooling step to T_n) demagnetizes gradually over the range T_0 to T_{n+1} in heating (field $H = 0$: first heating/cooling step to T_{n+1}). Temperature variation due to $M_s(T)$ has been removed. A pTRM residual remains after the T_{n+1} heating, contaminating the NRM. A larger residual would remain if heating were stopped at T_n (i.e. a third heating/cooling to T_n in zero field). This pTRM residual (T_n) is a pTRM tail check (Riisager et al., 2000).

and $f(T_{UB})$ distributions of the 110 and 135 μm magnetites in Figs. 2 and 3 originate in this way. The effect on paleointensity determination is a large loss of NRM in the low-temperature demagnetization steps, largely unmatched by gain in pTRM in the companion in-field steps (lower dashed curve in Fig. 4). Only in higher temperature steps when the NRM has dropped to ≈30% of its initial intensity does pTRM acquisition begin to outstrip NRM loss.

Simulated Thellier paleointensity experiments carried out on the present samples give a range of curves, all lying below the ideal SD line. The 135 μm data most closely approach the predictions of MD field blocking theory (Dunlop and Xu, 1994; Xu and Dunlop, 1994); the 1 μm data are closest to the SD line; the other grain sizes form a regular progression between them. The MD effect, i.e. $T_{UB} < T_B$, is important throughout the PSD range. Even for the 1 μm sample, the initial slope defined by the first five or six double-heatings overestimates the "paleofield" intensity by about 20%. Levi (1977) found similar results for 2.7 μm and smaller magnetites.

The high-temperature tail of $f(T_{UB})$, i.e. $T_{UB} > T_B$, also affects paleointensity determination. In double heatings at higher T, the NRM lost at T_n is more than replenished by pTRM gained in the second step. However, in the zero field heating step to the next higher temperature T_{n+1}, not all of the pTRM acquired at T_n is erased. The process is sketched in Fig. 5. For simplicity, imagine that pTRM is acquired sharply at $T_B = T_n$ (labeled "field H on"). Although there is only one value of T_B for pTRM (T_n), there is a continuum of T_{UB}, both $<T_n$ and $>T_n$ (demagnetization curve, labeled "field $H = 0$", extending from T_0 to T_C). The pTRM is not completely eliminated by heating to T_{n+1}. On cooling to T_0, there remains a pTRM residual (T_{n+1}), which contaminates the NRM.

In practical paleointensity work, there are a number of clues to watch for. If the laboratory field $\boldsymbol{H}$ is applied at a large angle to the NRM, the NRM direction will shift progressively towards $\boldsymbol{H}$ as pTRM residuals accumulate. If $\boldsymbol{H}$ is more or less parallel (or antiparallel) to the NRM, this clue is absent, but the

NRM intensity may ultimately increase to such an extent that the Arai plot curve climbs above the ideal SD line. The increase will depend on the number of residuals added; in Fig. 4, with 12–14 heating steps, points remain below the SD line. The surest indicator is a "pTRM tail check" (Riisager et al., 2000), best performed as a third zero-field heating–cooling step at T_n, before proceeding to heatings and coolings at T_{n+1}. Any undemagnetized residual at T_n is immediately obvious. The residual at T_{n+1} would of course be smaller (see Fig. 5) but probably not zero.

Counterintuitively, pTRM tail checks are best done at intermediate temperatures. The reason is that as $T_n \rightarrow T_C$, there is a limited temperature range in which a high T_{UB} tail can form, whereas at intermediate temperatures, there is a large range from T_n to T_C available.

6. Pre-treatments to improve PSD thermal demagnetization behavior

Two treatments were carried out prior to thermal demagnetization of pTRM of the 20 μm sample in an attempt to reduce the low- and high-T_{UB} tails of $f(T_{UB})$. The first was low-temperature demagnetization (LTD), consisting of zero-field cooling through the isotropic point (130 K) and Verwey transition (120 K) of magnetite, followed by zero-field warming to T_0. LTD reduced the loss of remanence between T_0 and 300°C in subsequent thermal demagnetization to ≈10%, compared to ≈25% for the untreated pTRM (Fig. 6). On the other hand, the fraction of pTRM with $T_{UB} > 400$°C was not removed in the same proportion (although the experiments are not analogs, Shcherbakova et al. (1996) found that low-T_B pTRMs were more vulnerable to LTD than high-T_B pTRMs).

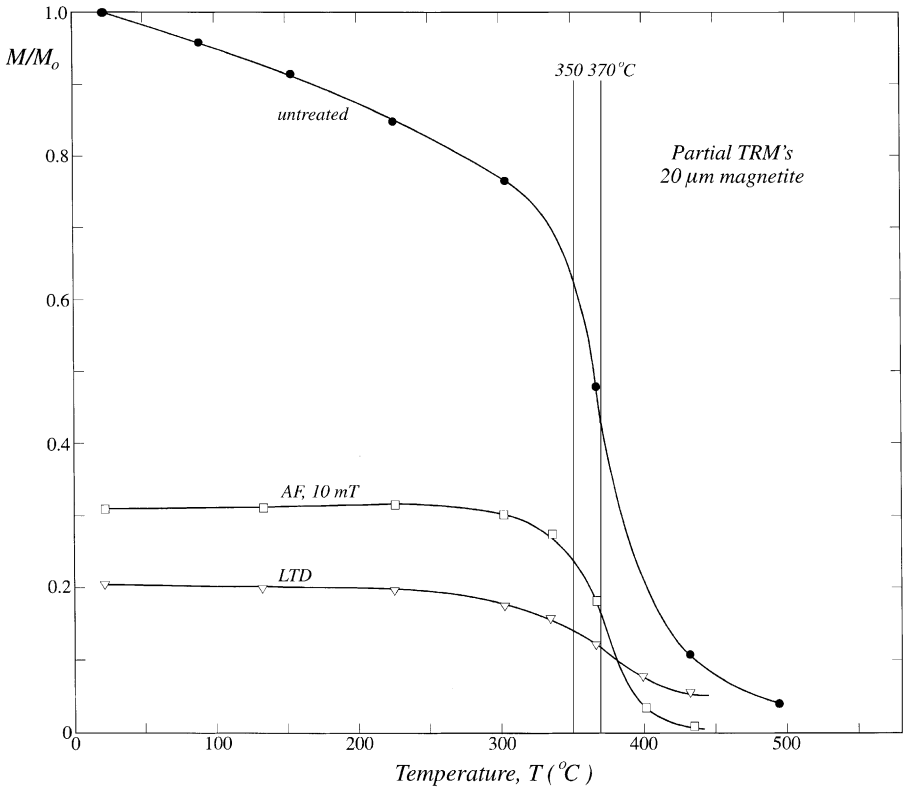

Fig. 6. The effect of AF and LTD pre-treatments on subsequent thermal demagnetization of pTRM for the 20 μm sample. Magnetization is normalized to pTRM intensity before AF or LTD cleaning. AF is the more effective treatment, removing almost all remanence with T_{UB} outside the 300–400°C range.

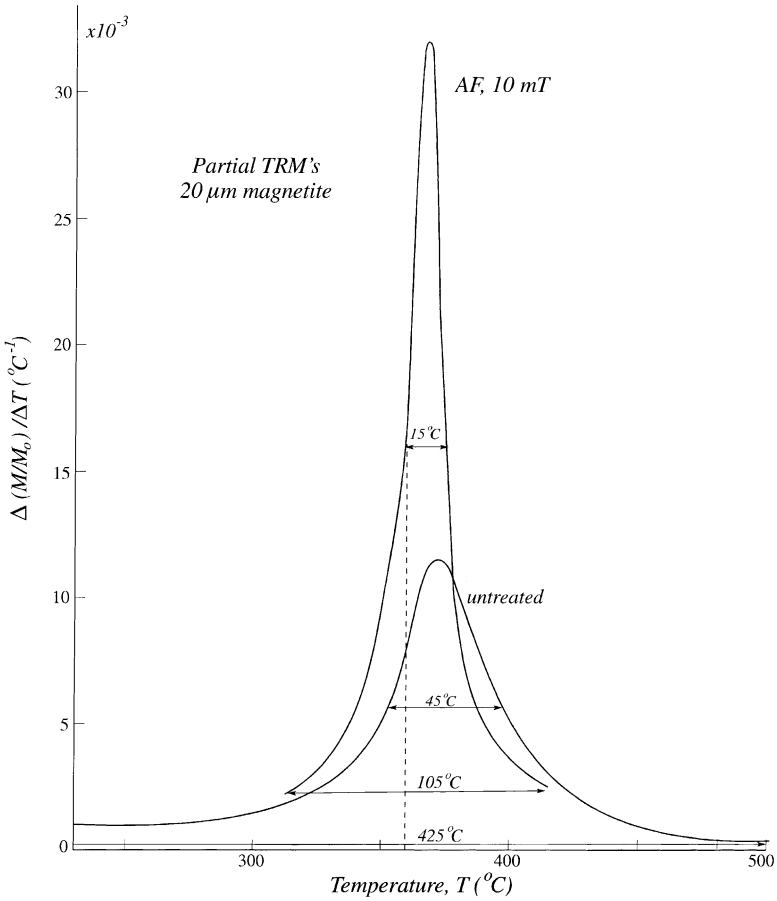

Fig. 7. Unblocking temperature distributions $f(T_{UB})$ obtained by numerically differentiating the thermal demagnetization curves of Fig. 6. The distribution is sharpened by AF pre-treatment (half-width reduced from 45 to 15°C) and low and high T_{UB} tails are eliminated (95–5% range reduced from 425 to 105°C). Here magnetization is normalized to post-AF remanence for the AF spectrum, whereas in Fig. 6 normalization was to untreated pTRM.

Overall, only 20% of the pTRM remained after LTD, reducing the signal to be measured by almost an order of magnitude.

Partial alternating field (AF) demagnetization to a peak field of 10 mT was more successful. About 30% of the pTRM remained, and when heated, it was virtually unaffected up to 300°C. On the high temperature side, the pTRM was reduced to 3% by 400°C and to <1% by 430°C. Thus, the unblocking temperature range was reduced about equally above and below the blocking range.

The effectiveness of AF pre-treatment is clear in the corresponding $f(T_{UB})$ spectra (Fig. 7). The spectral half-width of the untreated pTRM is 45°C and the tails are extremely broad: a spread of 425°C between the 5 and 95% limits of the distribution. After 10 mT, AF treatment, $f(T_{UB})$ is sharply peaked, with a half-width of 15°C, and 90% of the remanence unblocks within a 105°C range roughly centered on $(T_B)_{av} = 360$°C.

7. Discussion

7.1. Principal findings

The new features of this work are: (1) partial TRM produced over a narrow temperature interval, i.e. representing essentially a single T_B, has a wide distri-

bution of unblocking temperatures T_{UB}; (2) low unblocking temperatures ($T_{UB} < T_B$) are as prevalent as high unblocking temperatures; (3) the high- and low-T_{UB} tails of the distribution $f(T_{UB})$ are roughly symmetric, leading to a mean unblocking temperature $(T_{UB})_{av} \approx T_B$. These properties were previously established for VRM produced at similar temperatures (Dunlop and Özdemir, 2000), for one PSD and one MD sample (20 and 135 μm, respectively). The present work uses a wider range of PSD and MD grain sizes, and demonstrates a regular progression of thermal demagnetization characteristics, from limited tails and a concentration of T_{UB} in a ≈40°C range around T_B for 1 and 6 μm magnetites, to very broadly distributed T_{UB} in 100–125 and 125–150 μm magnetites (Figs. 2 and 3).

The 20 μm sample is particularly interesting because its $f(T_{UB})$ combines an SD-like central peak with broad MD-like tails. The superposition of spectra implies coexisting but independent SD- and MD-like processes in PSD grains of this size. There has been much speculation about the nature of PSD remanence, dating back to Verhoogen (1959) and Stacey (1962), but little hard evidence for the independence of SD and MD moments.

Shcherbakova et al. (2000) concluded that pTRM thermal demagnetization tails are relatively minor for PSD grains. It is certainly the case that large MD grains, such as the 110 and 135 μm magnetites of the present study, have the broadest distributions and most prominent demagnetization tails. However, the pTRM of 20 μm and even 6 and 1 μm magnetites undergo 50% or more of their unblocking below and above the pTRM blocking range of 370–350°C (Fig. 2). They have clear tails in $f(T_{UB})$ spectra, particularly for $T_{UB} < T_B$ (Fig. 3). The low-T_{UB} tails lead to curved Arai plots that deviate sufficiently from an ideal SD line to seriously compromise paleointensity determinations in this size range (Fig. 4).

Shcherbakova et al. (2000) also concluded that pTRM thermal demagnetization tails are dependent on initial state, being largest when a sample is heated in zero field to T_C and cooled in zero field to the upper pTRM temperature T_1 (a thermally cooled or TC initial state). A thermally heated (TH) initial state, in which the sample is first thermally demagnetized by heating to T_C and back to T_0 and then heated in zero field to T_1, resulted in a smaller pTRM tail above T_1.

We examined VRM acquired by the 135 μm sample at 350°C from three different initial states, TC, TH and AF demagnetized. All display prominent low-T tailing in their thermal demagnetization curves, although the high-T trends are indeterminate because of noise at low-remanence levels (Fig. 8). The TC initial state leads to the largest tail, but the TH and AF states also have associated tails. A similar trend appears in thermal demagnetization data by Halgedahl (1993).

In a Thellier experiment, pTRMs are produced from a TC initial state, whereas most of the pTRMs in the present study had an AF initial state. Fig. 8 implies that deductions about behavior in paleointensity determination (e.g. Fig. 5 and Section 5) based on our pTRM thermal demagnetization data probably underestimate deviations from ideal SD behavior. The data of Fig. 4 are of course experimental and not subject to any such uncertainty.

7.2. Consequences of "anomalously" high and low unblocking temperatures

Middleton and Schmidt (1982), Dunlop (1983), Kent (1985), and Jackson and Van der Voo (1986) found that both laboratory VRMs and geological thermoviscous overprints were more resistant to thermal demagnetization than predicted by Néel's SD theory, as embodied in the time–temperature relations of Pullaiah et al. (1975). A geological restudy, with attention to the domain state of individual samples (Dunlop et al., 1997), and laboratory studies of thermal demagnetization of VRM (Dunlop and Özdemir, 1993, 2000) have made it clear that SD grains do demagnetize sharply at or very near T_B but PSD and MD grains must be heated to higher temperatures to completely erase the remanence. Figs. 2 and 3 show how demagnetization tails increase in importance as grain size increases above SD through the magnetite PSD range to truly MD sizes.

High-temperature tails have practical consequences in the stepwise thermal demagnetization of NRMs that are a composite of a primary NRM partly overprinted and replaced by secondary magnetization. Multivectorial NRMs of this type are the norm in all but very young and completely undisturbed rocks. Such composites are sometimes difficult to resolve cleanly, a problem that is often ascribed to chemical rather than thermal or thermoviscous remagnetization. In reality,

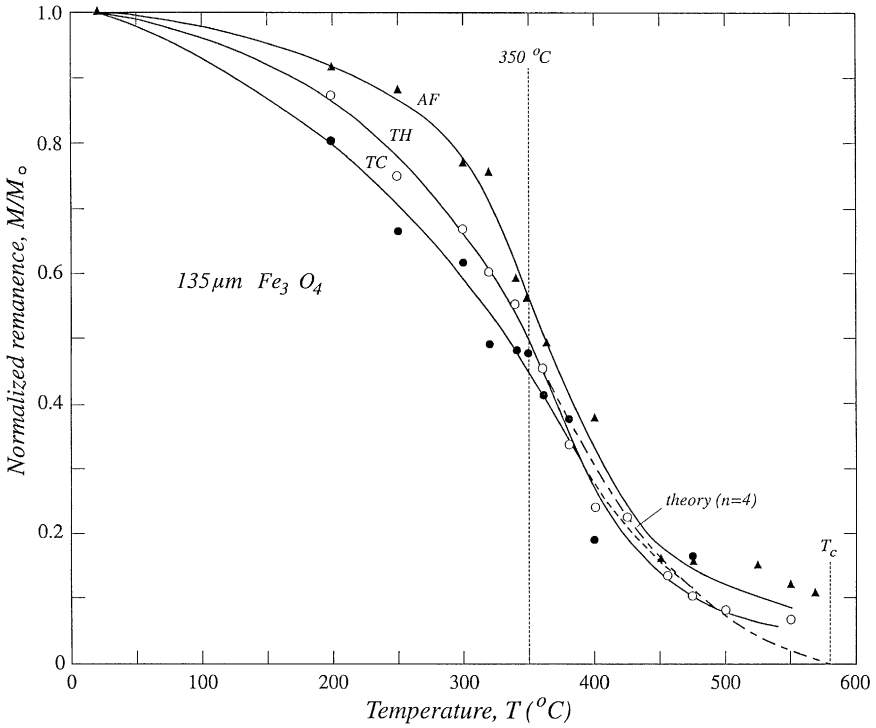

Fig. 8. A test of the effect of initial state before acquisition of VRM (350°C, 3.5 h, 135 μm grains) on subsequent thermal demagnetization behavior. Although the thermally cooled (TC) state leads to the largest low-T_{UB} tail, the thermally heated (TH) and AF states also have substantial fractions of both "anomalously low" and "anomalously high" T_{UB}'s. The dashed curve results from the thermal demagnetization theory of Xu and Dunlop (1994), based on repeated wall jumps during heating as in Néel's (1955) theory of MD TRM.

one would only anticipate a clean separation for SD grains and perhaps the very smallest of PSD grains, and these are rare in nature. Physics (non-SD domain states), not chemistry, may be the culprit when multivectorial remanences fail to separate cleanly in thermal treatment.

Thellier-type paleointensity experiments generate a laboratory superposition of "primary" NRM and overprinting pTRM. For the success of the experiment, it is vital that each successive pTRM overlay be totally erased before the next pTRM is produced. Undemagnetized pTRM residuals from prior heatings will contaminate the NRM (Fig. 5). They may be recognizable by the deflection they cause in the vector direction of the contaminated NRM, if the NRM and pTRM axes are sufficiently oblique to each other.

A more foolproof test is a "pTRM tail check" (Riisager et al., 2000), which unfortunately adds one more heating–cooling step at each temperature. If pTRM tail checks are planned, they should begin at moderate temperatures because the importance of high-T tails depends in part on the breadth of the temperature range available below T_C. Shcherbakova et al. (2000) have noted that the importance of pTRM tails in individual samples depends on the blocking temperature interval of the pTRM. Partial TRMs produced at 500°C and above, just below T_C, had less prominent tails than pTRMs produced around 300 or 400°C, for which a much wider temperature range below T_C is available.

"Anomalously" low unblocking temperatures have equally serious consequences (Fig. 4). Because of the symmetry of the $f(T_{UB})$ distribution, during roughly the first half of a paleointensity experiment, the unblocking of NRM outweighs the blocking of pTRM; during the second half, pTRM blocking begins to catch up with NRM demagnetization, ultimately restoring points on an Arai plot to the ideal SD line just before the ultimate demagnetization of the sample. The result is a characteristic sagging shape of paleointensity results, the amount of sagging growing for larger

grain sizes. If this intrinsic concave shape is mistakenly taken to be due to chemical alteration in high-temperature steps and a line is fitted to the low-temperature points, paleointensity estimates that are high by ≈20% for 1 μm grains or >50% for 135 μm grains will result. It remains to be seen whether pTRM checks can reliably distinguish between the two causes of curvature.

7.3. Consequences of the symmetry of $f(T_{UB})$

A more sophisticated application of SD theory to thermoviscous overprinting in nature is thermochronometry (Middleton and Schmidt, 1982; Dunlop et al., 1997, 2000). As discussed above, "anomalously" high unblocking temperatures, i.e. $T_{UB} > T_B$, due to MD or PSD grains invalidate the simple prescription $T_{UB} = T_B$, based on SD theory, by which paleotemperatures are matched to laboratory unblocking temperatures (Pullaiah et al., 1975). Some form of preconditioning, such as LTD or partial AF cleaning (Fig. 6), may improve the situation by reducing high-T_{UB} tails.

A more satisfying solution would be to take advantage of the symmetry of $f(T_{UB})$. Since $(T_{UB})_{av} \approx T_B$ for individual narrow-band pTRMs, using average instead of maximum unblocking temperatures would in principle solve the problem whatever the domain state of remanence carriers. Implementing this principle is not straightforward, however, because the $f(T_{UB})$ distributions of the various narrow-band pTRMs comprising the thermal overprint overlap. The upper tail of one overlaps the lower tail of another, leading to a wide and fairly uniform spectrum of T_{UB}.

On the other hand, the overlap of the $f(T_{UB})$ distributions of adjacent pTRMs suggests an application to the law of additivity of partial TRMs. Clearly adjacent pTRMs carried by MD or PSD grains cannot be independent because their unblocking temperature ranges overlap, sometimes extensively. Yet it is a common observation (Roquet, 1954; Levi, 1979) that PSD and even MD pTRM intensities are additive:

$$\mathrm{pTRM}(T_1, T_2, H) + \mathrm{pTRM}(T_2, T_3, H) = \mathrm{pTRM}(T_1, T_3, H) \quad (1)$$

Furthermore, this additivity holds throughout the thermal demagnetization process, as the data in Fig. 9 illustrate. Two broad-band pTRMs were used because the higher remanence intensities greatly improved the precision of the measurements. The shapes of the thermal demagnetization curves of pTRM (T_C, 300°C) and pTRM (300°C, T_0) are quite different, but they sum to give, to a good approximation, the same curve

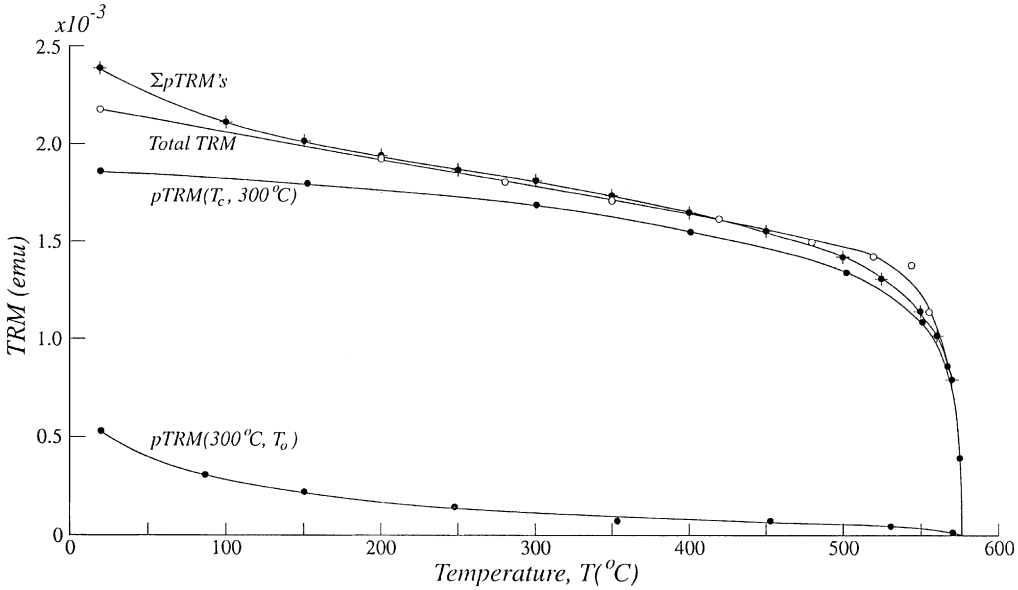

Fig. 9. Additivity of broad-band pTRMs produced over neighboring intervals together spanning the range (T_C, T_0). At any temperature between about 100 and 500°C, the two thermal demagnetization curves sum to the same value as the total TRM demagnetization curve.

as the thermal demagnetization of the total TRM. The two pTRMs account for different fractions of the sum at different temperatures, but the mirror symmetry of their $f(T_{UB})$ spectra about their common blocking temperature of 300°C is responsible for the constancy of the sum.

7.4. Fundamental considerations

Two fundamental questions spring to mind. First, why are the high- and low-T tails of $f(T_{UB})$ symmetric? This symmetry for narrow-band pTRMs (Figs. 1, 3 and 7) accounts also for the mirror symmetry of $f(T_{UB})$ for adjacent broad-band pTRMs, by which the upper tail of one matches the lower tail of the other, resulting in a constant sum of the two pTRMs during thermal demagnetization (Fig. 9). Second, why are the tails of $f(T_{UB})$ selectively erased by partial AF demagnetization, sharpening the distribution (Fig. 7)? Are the same domain nucleation events or wall displacements that occur far below and far above T_B during heating selectively excited by AF treatment at room temperature?

Nucleation and growth of a new domain must profoundly alter the internal demagnetizing field H_d at every point in a grain and can be expected to trigger a cascade of adjustments in other domains. Wall displacements, on the other hand, are a local response to gradual changes in H_d. When H_d becomes greater than the pinning strength of a local obstacle to wall motion, a segment of the wall will snap free and move a small distance, limited by other pins along the wall. Nucleation is an infrequent but profound event with global consequences throughout the grain, while wall displacement is a local effect that occurs frequently and changes the grain's magnetization quasi-continuously, driven by the continuously changing balance between H_d and coercivity H_c, representing wall pinning, as temperature changes.

Nucleation occurs at specific sites where the crystalline anisotropy K is anomalously low (sharp corners, interior cavities) and spins can be more readily reversed by H_d. Intuitively we might expect nucleation to be most probable in two temperature ranges: at low T where K is decreasing rapidly with heating and at high T near T_C where H_d outweighs all sources of coercivity. The observations on magnetite support this idea. Heider et al. (1988) observed successive nucleation events at a sharp corner in heating to ≈120°C with few changes in further heating, while Ambatiello et al. (1999) have reported constant domain sizes until crystals were heated above ≈450°C.

On this evidence, nucleation has the right properties to contribute disproportionately to high- and low-T_{UB} tails in pTRM demagnetization. However, it is not credible that these same nucleation events can be produced by AF cleaning in small fields ≤10 mT at T_0. It is much more likely that displacements of loosely pinned walls account for the softest AF fraction and nucleation events for much higher coercivity fractions.

Re-examining the data in Fig. 6, we see that although the pTRM fractions with $T_{UB} < 300$°C and >400°C are most vulnerable to AF pre-treatment, the pTRM fraction with 300°C < T_{UB} < 400°C is also greatly reduced, from ≈60% of the original pTRM without AF to ≈30% after AF cleaning. In other words, AF demagnetization affects the entire $f(T_{UB})$ spectrum. The AF pre-treatment is selective in the sense that only pTRM with T_{UB} between 300 and 400°C survives to any significant extent, but the fractions of the original pTRM destroyed are actually heavily weighted towards the 300–400°C interval: 30% in this 100°C interval compared to 20% in the 280°C interval from 20 to 300°C and 20% in the 180°C interval from 400°C to T_C. Successive wall displacements over the entire interval from T_0 to T_C are the likely source of this AF vulnerable fraction.

Fig. 1 gives further insight. The distribution $f(T_{UB})$ for the 20 μm sample is a superposition of a narrow, sharply peaked spectrum like that of the 0.04 μm SD sample and a very broad spectrum like that of the 135 μm MD sample. What AF demagnetization has accomplished is to erase the MD spectrum (which does indeed peak around the blocking range, accounting for the larger fraction of pTRM destroyed between 300 and 400°C), leaving the SD-like spectrum untouched.

If wall displacements occurring more or less uniformly across the entire range of heating are the predominant mechanism of thermal demagnetization, as the above analysis implies, the symmetry of $f(T_{UB})$ becomes easier to understand. If T_B is in a mid-temperature range between T_0 and T_C, as in our experiments, there is a symmetric range of T available for demagnetization above and below T_B. By this reasoning, experiments involving very low-T_B pTRM would be expected to show a reduced low-T_{UB} tail and very high-T_B pTRM should have a reduced high-T_{UB} tail.

The latter effect has been observed by Shcherbakova et al. (2000).

8. Conclusions

1. Narrow-band pTRMs produced during cooling by a field applied in the interval 370–350°C to PSD and MD magnetites with mean sizes of 1, 6, 20, 110 and 135 μm were not demagnetized over the same interval during heating. Thermal demagnetization began well below 350°C and continued above 370°C. However, the median unblocking temperature $(T_{UB})_{av}$ was close to the median blocking temperature $(T_B)_{av}$ of 360°C in all cases.
2. The MD samples (110 and 135 μm) deviated most from SD behavior. Their pTRMs demagnetized over the entire interval (T_0, T_C).
3. The PSD samples (1, 6 and 20 μm) had thermal demagnetization curves with pronounced inflections near the lower and upper limits of the pTRM blocking range. Although 60–80% of the pTRM demagnetized between 300 and 400°C, there were also important "tails" below 300 and above 400°C.
4. The combination of SD- and MD-like thermal demagnetization behavior in PSD grains is most clearly seen in the unblocking temperature distribution, $f(T_{UB})$, the point-by-point slope of the thermal demagnetization curve. PSD grains have a non-Gaussian distribution that is a superposition of separate narrow SD-like and broad MD-like distributions. The superposition implies independent SD-like and MD sources of remanence in these grains.
5. "Anomalously" low unblocking temperatures, i.e. $T_{UB} < T_B$, affect Thellier-type paleointensity determination because demagnetization of NRM in low-temperature steps is not offset by the gain in pTRM in the companion in-field heating–cooling steps. As a result, the Arai plot sags below the ideal SD line (Fig. 4). Mistaken use of only low-temperature steps would lead to paleointensity estimates that are high by ≈20% for 1 μm grains up to a factor 2 high for 135 μm grains.
6. "Anomalously" high unblocking temperatures of PSD and MD grains, i.e. $T_{UB} > T_B$, invalidate the determination of paleotemperatures using thermoviscous remagnetizations (Pullaiah et al., 1975) because the method is based on Néel's SD theory and assumes $T_{UB} = T_B$ (apart from a cooling rate correction). The use of $(T_{UB})_{av}$ values would revalidate the method, because $(T_{UB})_{av} \approx T_B$ for narrow-band pTRMs, but for the broad-band pTRMs that constitute NRM overprints, this may be difficult to implement.
7. High T_{UB}'s also lead to pTRM residuals in intermediate- and high-T steps of paleointensity experiments, best detected by an additional zero-field heating–cooling cycle at each temperature (pTRM tail check).
8. Since $f(T_{UB})$ of a broad-band pTRM results from the superposition of $f(T_{UB})$ of many narrow-band pTRMs, the symmetry of $f(T_{UB})$ for individual narrow-band pTRMs leads to a mirror-image symmetry of thermal demagnetization tails of neighboring broad-band pTRMs. As a result, at any thermal demagnetization temperature, the sum of the two pTRMs equals the total TRM, an unanticipated extension of the law of additivity of pTRMs (Fig. 9).
9. AF cleaning to 10 mT renders the surviving pTRM of 20 μm PSD grains much more SD-like in its thermal demagnetization behavior. Essentially all the surviving pTRM unblocks between 300 and 400°C. The MD-like part of $f(T_{UB})$, surmised to be due to repeated wall jumps, is completely removed by this mild AF treatment.

Acknowledgements

We thank Valera Shcherbakov, Andrei Kosterov and Michel Prévot for constructive reviews and suggestions and Yong Jae Yu for discussions about pTRM tail checks. Many of our experiments were carried out at the Institute for Rock Magnetism (IRM), University of Minnesota, with help and encouragement from Jim Marvin, Mike Jackson, Subir Banerjee and Bruce Moskowitz. The IRM is operated with support from the National Science Foundation, the Keck Foundation, and the University of Minnesota. The work of the University of Toronto rock magnetism group is supported by grants from the Natural Sciences and Engineering Research Council of Canada.

References

Ambatiello, A., Fabian, K., Hoffmann, V., 1999. Magnetic domain structure of multidomain magnetite as a function of temperature:

observation by Kerr microscopy. Phys. Earth Planet. Inter. 112, 55–80.

Bol'shakov, A.S., Shcherbakova, V.V., 1979. A thermomagnetic criterion for determining the domain structure of ferromagnetics (English translation). Izv. Phys. Solid Earth 15, 111–117.

Dunlop, D.J., 1983. Viscous magnetization of 0.04–100 μm magnetites. Geophys. J. R. Astron. Soc. 74, 667–687.

Dunlop, D.J., 1998. Thermoremanent magnetization of non-uniformly magnetized grains. J. Geophys. Res. 103, 30561–30574.

Dunlop, D.J., Özdemir, Ö., 1993. Thermal demagnetization of VRM and pTRM of single domain magnetite: no evidence for anomalously high unblocking temperatures. Geophys. Res. Lett. 20, 1939–1942.

Dunlop, D.J., Özdemir, Ö., 2000. Effect of grain size and domain state on thermal demagnetization tails. Geophys. Res. Lett. 27, 1311–1314.

Dunlop, D.J., West, G.F., 1969. An experimental evaluation of single domain theories. Rev. Geophys. 7, 709–757.

Dunlop, D.J., Xu, S., 1994. Theory of partial thermoremanent magnetization in multidomain grains. 1. Repeated identical barriers to wall motion (single microcoercivity). J. Geophys. Res. 99, 9005–9023.

Dunlop, D.J., Özdemir, Ö., Schmidt, P.W., 1997. Paleomagnetism and paleothermometry of the Sydney Basin. 2. Origin of anomalously high unblocking temperatures. J. Geophys. Res. 102, 27285–27295.

Dunlop, D.J., Özdemir, Ö., Clark, D.A., Schmidt, P.W., 2000. Time–temperature relations for the remagnetization of pyrrhotite (Fe_7S_8) and their use in estimating paleotemperatures. Earth Planet. Sci. Lett. 176, 107–116.

Everitt, C.W.F., 1961. Thermoremanent magnetization. I. Experiments on single domain grains. Phil. Mag. 6, 713–726.

Everitt, C.W.F., 1962. Thermoremanent magnetization. II. Experiments on multidomain grains. Phil. Mag. 7, 583–597.

Halgedahl, S.L., 1991. Magnetic domain patterns observed on synthetic Ti-rich titanomagnetite as a function of temperature and in states of thermoremanent magnetization. J. Geophys. Res. 96, 3943–3972.

Halgedahl, S.L., 1993. Experiments to investigate the origin of anomalously elevated unblocking temperatures. J. Geophys. Res. 98, 22443–22460.

Heider, F., Halgdahl, S.L., Dunlop, D.J., 1988. Temperature dependence of magnetic domains in magnetite crystals. Geophys. Res. Lett. 15, 499–502.

Jackson, M., Van der Voo, R., 1986. Thermally activated viscous remanence in some magnetite- and hematite-bearing dolomites. Geophys. Res. Lett. 13, 1434–1437.

Kent, D., 1985. Thermoviscous remagnetization in some Appalachian limestones. Geophys. Res. Lett. 12, 805–808.

Levi, S., 1977. The effect of magnetite particle size on paleointensity determinations of the geomagnetic field. Phys. Earth Planet. Inter. 13, 245–259.

Levi, S., 1979. The additivity of partial thermal remanent magnetization in magnetite. Geophys. J. R. Astron. Soc. 59, 205–218.

Markov, G.P., Shcherbakov, V.P., Bol'shakov, A.S., Vinogradov, Yu.K., 1983. On the temperature dependence of the partial thermoremanent magnetization of multidomain grains (English translation). Izv. Phys. Solid Earth 19, 625–630.

McClelland, E., Shcherbakov, V.P., 1995. Metastability of domain state in multidomain magnetite: consequences for remanence acquisition. J. Geophys. Res. 100, 3841–3857.

McClelland, E., Sugiura, N., 1987. A kinematic model of TRM acquisition in multidomain magnetite: consequences for remanence acquisition. Phys. Earth Planet. Inter. 46, 9–23.

McClelland, E., Muxworthy, A.R., Thomas, R.M., 1996. Magnetic properties of the stable fraction of remanence in large multidomain (MD) magnetite grains: single-domain or MD? Geophys. Res. Lett. 23, 2831–2834.

Middleton, M.F., Schmidt, P.W., 1982. Paleothermometry of the Sydney basin. J. Geophys. Res. 87, 5351–5359.

Muxworthy, A.R., 2000. Cooling behaviour of partial thermoremanences induced in multidomain magnetite. Earth Planet. Sci. Lett. 184, 169–179.

Néel, L., 1949. Théorie du traînage magnétique des ferromagnétiques en grain fins avec applications aux terres cuites. Ann. Géophys. 5, 99–136.

Néel, L., 1955. Some theoretical aspects of rock magnetism. Adv. Phys. 4, 191–243.

Pullaiah, G., Irving, E., Buchan, K.L., Dunlop, D.J., 1975. Magnetization changes caused by burial and uplift. Earth Planet. Sci. Lett. 28, 133–143.

Riisager, J., Perrin, M., Riisager, P., Ruffet, G., 2000. Paleomagnetism, paleointensity and geochronology of Miocene basalts and baked sediments from Velay Oriental, French Massif Central. J. Geophys. Res. 105, 883–896.

Roquet, J., 1954. Sur les rémanences magnétiques des oxydes de fer et leur intérêt en géomagnétisme. Ann. Géophys. 10, 226–247, 282–325.

Shaskanov, V.A., Metallova, V.V., 1972. Violation of Thellier's law for partial thermoremanent magnetizations (English translation). Izv. Phys. Solid Earth 8, 180–184.

Shcherbakov, V.P., McClelland, E., Shcherbakova, V.V., 1993. A model of multidomain thermoremanent magnetization incorporating temperature-variable domain structure. J. Geophys. Res. 98, 6201–6216.

Shcherbakova, V.V., Shcherbakov, V.P., Schmidt, P.W., Prévot, M., 1996. On the effect of low-temperature demagnetization on TRMs and pTRMs. Geophys. J. Int. 127, 379–386.

Shcherbakova, V.V., Shcherbakov, V.P., Heider, F., 2000. Properties of partial thermoremanent magnetization in PSD and MD magnetite grains. J. Geophys. Res. 105, 767–781.

Stacey, F.D., 1962. A generalized theory of thermoremanence, covering the transition from single domain to multi-domain magnetic grains. Phil. Mag. 7, 1887–1900.

Verhoogen, J., 1959. The origin of thermoremanent magnetization. J. Geophys. Res. 64, 2441–2449.

Worm, H.-U., Jackson, M., Kelso, P., Banerjee, S.K., 1988. Thermal demagnetization of partial thermoremanent magnetization. J. Geophys. Res. 93, 12196–12204.

Xu, S., Dunlop, D.J., 1994. Theory of partial thermoremanent magnetization in multidomain grains. 2. Effect of microcoercivity distribution and comparison with experiment. J. Geophys. Res. 99, 9025–9033.